

RESEARCH

Open Access



# The effects of multiple environmental factors on global carbon allocation

Jiangzhou Xia<sup>1</sup> , Yang Chen<sup>1\*</sup>, Wenping Yuan<sup>2\*</sup> and Ying-Ping Wang<sup>3</sup>

## Abstract

**Background** The allocation of photosynthate among the parts of plants (e.g., leaves, wood tissues and roots) strongly regulates their growth, and this conditions the terrestrial carbon cycle. Recent studies have shown that atmospheric CO<sub>2</sub> and climate change dominate the changes in carbon allocation in plants, but the magnitude and mechanism of its effects remain unclear.

**Methods** The Community Atmosphere Biosphere Land Exchange (CABLE) model can accurately simulate the responses of carbon allocation to environmental changes. This study quantifies the contributions of four environmental factors—atmospheric CO<sub>2</sub>, temperature, precipitation, and radiation—on resource availability and carbon allocation from 1979 to 2014 by using the CABLE model.

**Results** The results of the CABLE model showed that rising CO<sub>2</sub> significantly reduced carbon allocation to the leaves of plants at a global scale, but the other three environmental factors exhibited contrasting effects that dominated the rise in carbon allocation to the leaves. The increased precipitation and CO<sub>2</sub> significantly reduced the light availability and increased carbon allocation to the wooden parts of plants. By contrast, the rising temperature reduced the water availability, resulting in a decrease in carbon allocation to the wooden parts. All four environmental factors consistently exhibited negative effects on carbon allocation to the roots, with rising precipitation causing the largest reduction in carbon allocation to them. Moreover, except for CO<sub>2</sub>, the effects of the other three environmental factors were heterogeneous owing to their variable interactions in different regions.

**Conclusions** The CABLE model can accurately represent the mechanisms of response of resource availability and carbon allocation to environmental changes. Our study highlights the substantial environmental regulation of global carbon allocation. The responses of carbon allocation to global environmental changes need to be extensively studied through ecosystem models based on different hypotheses.

**Keywords** Carbon allocation, CO<sub>2</sub>, Temperature, Precipitation, Radiation, Terrestrial ecosystem model

## Background

Carbon allocation, or the allocation of photosynthate among the parts of plants (e.g., leaves, wood tissues and roots), is one of the most important physiological processes in nature (Xia et al. 2019; Sierra et al. 2022). It determines not only plant growth, but also numerous processes of the ecosystem, including decomposition, carbon and nitrogen sequestration, and the exchange of water between plants and the atmosphere (Aber and Melillo 1991). The carbon allocated to the woody tissues of plants has a longer residence time than that in their leaves or roots, where this significantly influences the

\*Correspondence:

Yang Chen  
cheny0323@163.com  
Wenping Yuan  
yuanwpcn@126.com

<sup>1</sup>Tianjin Key Laboratory of Water Resources and Environment, Tianjin Normal University, Tianjin 300387, China

<sup>2</sup>Institute of Carbon Neutrality, Sino-French Institute for Earth System Science, College of Urban and Environmental Sciences, Peking University, Beijing 100091, Beijing, China

<sup>3</sup>Commonwealth Scientific and Industrial Research Organization, Environment, Private Bag 10, Clayton South, VIC 3169, Australia

global carbon budget (Friedlingstein et al. 1999; McMurtrie and Dewar 2013; Xia et al. 2017; Wei et al. 2022). Carbon allocation between the wooden and non-wooden parts of plants also determines the quality and rate of decomposition of litter (Bird and Torn 2006). Ise et al. (2010) found a large variation in estimates of wooden biomass that stemmed from different assumptions about the coefficients of carbon allocation. The ratio of carbon allocated to the stems of plants in forests according to the vegetation integrative simulator for trace gases (VISIT) model was found to be higher than that of the Biome-BGC model (e.g., 0.517 vs. 0.3 for tropical forests), because of which the wooden biomass simulated by the former model was 178 Pg C higher than that of the latter (Ise et al. 2010). Therefore, reliable estimates of the changes in carbon allocation are crucial for reducing uncertainty in modeling the global carbon cycle.

Carbon allocation varies substantially over space and time in the context of global climate change, but the effects of climate change on carbon allocation are not well understood. For example, a rising CO<sub>2</sub> concentration has exhibited divergent effects on carbon allocation in two long-term experiments on CO<sub>2</sub> enrichment—an increase in carbon allocation to the wooden parts of plants at Duke but a decrease in it at Oak Ridge—as a result of the different responses of the availability of nitrogen in soil to CO<sub>2</sub> enrichment (De Kauwe et al. 2014). Moreover, previous studies have highlighted the inconsistent responses of carbon allocation to the components of plants under warming conditions. Warmer climate has been reported to increase the NPP in boreal forests but reduce the growth of wood, while the limitation in nutrients resulting from rising temperatures leads to greater carbon allocation to the roots (Lapenis et al. 2013). However, there is a dearth of research on how carbon allocation among the components of plants varies with different environmental variables at the global scale, where this is important for understanding the effects of carbon allocation on the terrestrial carbon budget (Xia et al. 2015; Wang et al. 2023).

The modeled response mechanism of carbon allocation to environmental changes remains unclear. Theoretically, the dynamic characteristics of plant carbon allocation result from their response in terms of using carbon to capture the most limiting resources (e.g., light, water, and nutrients) (Sharpe and Rykiel 1991; Kobe et al. 2010). The limitation of critical resources, such as water and nutrients, can enhance carbon allocation to the roots of plants to increase their uptake and alleviate resource deficits (Ikegami et al. 2007; Matzek 2011; Peng et al. 2017; Brunn et al. 2022). Previous studies have suggested that an increase in the ratio of biomass of the roots to that of the shoots may play an important role in the adaptation of plants to drought (Nelson et al. 2004). By contrast, the

limitation in the radiation absorbed by them increases carbon allocation to the leaves at the expense of that to the roots to increase absorption of incoming photosynthetically active radiation by them (Wang et al. 2006). Whether the observational data support the assumptions of these models of carbon allocation, and whether the modeled mechanism of the responses of plants to the processes of carbon allocation are correct still require further study.

In this study, we report five modeling experiments based on the Community Atmosphere Biosphere Land Exchange (CABLE) model to illustrate how carbon allocation varies with environmental variables. The objectives of this study are to (1) illustrate the effects of multiple environmental factors on resource availability and carbon allocation, and (2) reveal the response mechanisms of carbon allocation and resource availability to environmental changes according to the CABLE model.

## Methods

### CABLE model

The CABLE model is a global land-surface model that has been integrated with the CASA (Carnegie–Ames–Stanford approach)-CNP (carbon–nitrogen–phosphorous) model (CASA-CNP). This model can simulate the carbon, nitrogen, phosphorus, water, and energy cycles in terrestrial ecosystems (Wang et al. 2010; Zhang et al. 2011). Four phases of leaf phenology determine the growth and patterns of carbon allocation in leaves in the CABLE model. These are the phases of maximum and steady leaf growth, leaf senescence, and dormancy or no leaves. During the first phase, the ratio of carbon allocation to the leaves (aleaf) is set to 0.8, while those to the wood tissues (awood) and roots (aroot) are set to 0.1 for wooden plant functional types (PFTs), and zero and 0.2, respectively, for non-wooden PFTs. The ratios of carbon allocation (i.e., aleaf<sub>p2</sub>, awood<sub>p2</sub>, and aroot<sub>p2</sub>) in the second phase (phase 2) are calculated according to the resource limitation carbon allocation model. During the third and fourth phases, aleaf is set to zero while awood and aroot are calculated by using the allocation ratios of phase 2 ( $awood = awood_{p2} / (awood_{p2} + aroot_{p2})$ ,  $aroot = aroot_{p2} / (awood_{p2} + aroot_{p2})$ ). For evergreen PFTs, the leaf phenology and carbon allocation persist in phase 2 throughout the year.

During the phase of steady leaf growth (i.e., phase 2), the allocation of photosynthate among the components of plants in the CABLE model is regulated by the availability of light, water, and nitrogen (hereinafter called the resource limitation model). This model assumes that the greatest part of the gain in carbon is allocated to the component of the plant that most limits its growth (Fig. 1). If the availability of light is limiting its growth,

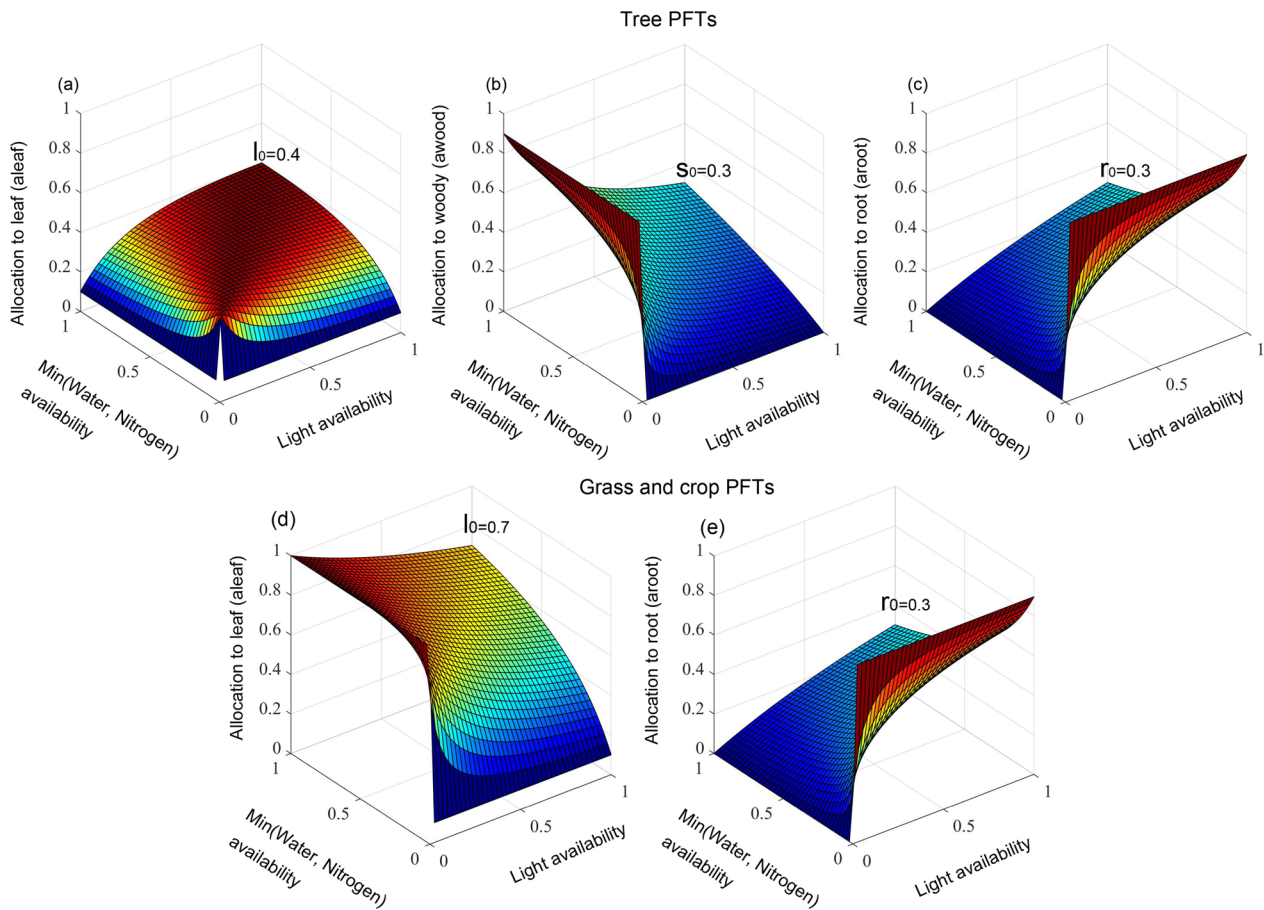


**Fig. 1** Fractions of allocation to the leaf (a), wood (b), and root (c) of the plant as functions of light (L), and the minimum values of the availability of water and nitrogen (Min(Water, Nitrogen)) for tree plant functional types (PFTs), with values of  $l_0=0.4$ ,  $s_0=0.3$ , and  $r_0=0.3$ . Fractions of allocation for the leaves (d) and roots (e) in grass and crop PFTs, with values of  $l_0=0.7$  and  $r_0=0.3$

the plant allocates more carbon to the wood tissues, such as stems. If water and nitrogen are limiting growth, the plant allocates more carbon to the roots (Fig. 1). The resource limitation carbon allocation model uses the scheme developed by Friedlingstein et al. (1999). The allocation coefficients of woody biomes for their leaves (aleaf), woody tissues (awood), and roots (aroot) are as follows:

$$aroot = 3r_0 \frac{L}{L + 2 \min(W, N)}, \tag{1}$$

$$awood = 3s_0 \frac{\min(W, N)}{2L + \min(W, N)}, \tag{2}$$

$$aleaf = 1 - awood - aroot. \tag{3}$$

For non-woody biomes, the allocation coefficients are as follows:

$$aroot = 3r_0 \frac{L}{L + 2 \min(W, N)}, \tag{4}$$

$$aleaf = 1 - aroot, \tag{5}$$

where  $\min(W, N)$  represents the minimum values of the availability of water (W) and nitrogen (N). The parameters  $r_0$  and  $s_0$  in the CABLE model describe the proportional allocation to the roots and wood tissues when resources are not limited. For the tree PFTs, both  $r_0$  and  $s_0$  are set to 0.3, with an allocation of 0.4 to the leaves ( $l_0$ ). For C3 grass and crop PFTs,  $r_0=0.3$  and  $l_0=0.7$  (Fig. 1).

Light availability (L) is calculated by:

$$L = \min[\max(e^{-0.5LAI}, 0), 1], \tag{6}$$

where LAI is the leaf area index.

Water availability (W) is calculated by:

$$W = \min[\max(\sum_{i=1}^n fr_i \frac{S_{wi} - S_{wilt}}{S_{field} - S_{wilt}}, 0), 1], \tag{7}$$

where  $fr_i$  is the fraction of root in the  $i$ th ( $n=6$ ) layer of soil,  $S_{wi}$  is the volumetric moisture content of soil in the  $i$ th layer, and  $S_{wilt}$  and  $S_{field}$  are the volumetric soil moisture contents at the wilting point and the field capacity soil moisture content, respectively.

Nitrogen availability ( $N$ ) is calculated as the product of the temperature of soil ( $T_s$ ) and moisture ( $W_s$ ) (Friedlingstein et al. 1999), where  $T_s$  is calculated based on a standard  $Q_{10}$  equation (Potter et al. 1993) and  $W_s$  is calculated by using Eq. (7):

$$N = T_s \times W_s, \tag{8}$$

$$T_s = Q_{10}^{\left(\frac{\sum_{i=1}^n fr_i T_{soil} - 30}{10}\right)}, \tag{9}$$

where  $T_{soil}$  ( $^{\circ}C$ ) is the temperature of soil in the  $i$ th layer, and  $Q_{10}=2.0$ .

The performance of the resource limitation carbon allocation scheme in CABLE model was evaluated at five natural observation sites and four global change manipulation experiments (precipitation reduction, warming, and elevated atmospheric  $CO_2$ ) in various ecosystems (Table 1 and Fig. 2b, Xia et al. 2017). The experiment at the C4 grass site in Oklahoma showed that the grass allocated more carbon to its roots under warming conditions. A precipitation control experiment at a rainforest site in Caxiuana showed that trees had decreased

values of awood, and increased values of aroot and aleaf under drought conditions. The elevated atmospheric  $CO_2$  ( $eCO_2$ ) experiment at the evergreen needleleaf tree at the Duke site showed that the tree allocated more carbon to wood under the  $eCO_2$  condition. The  $eCO_2$  experiment at the deciduous broadleaf tree of the Oak Ridge site showed that the tree allocated more carbon to the roots under the  $eCO_2$  condition. The CABLE was able to accurately simulate the responses of carbon allocation to environmental changes at those experimental sites (Xia et al. 2017). We thus used the CABLE model to explore the responses of plant carbon allocation to environmental changes (i.e., the dataset on precipitation, air temperature, and incident shortwave radiation obtained from the Modern-Era Retrospective Analysis for Research and Applications (MERRA), and data on atmospheric  $CO_2$  concentration).

#### Input data for CABLE model

The CABLE model was driven by the 1-hourly MERRA dataset (Global Modeling and Assimilation Office 2004), which contained data on the air temperature ( $T_{air}$ ), precipitation (Prec), specific humidity ( $Q_{air}$ ), incident longwave radiation (Lwd), incident shortwave radiation (Swd), pressure (Ps) and wind speed (Wind) from 1979 to 2014. The spatial resolution of the data was  $0.5^{\circ}$  latitude by  $0.67^{\circ}$  longitude. The annual mean  $CO_2$  concentration from 1850 to 2014 was obtained from research by Keeling and Whorf (2005). The fixed PFTs for 2005 were based on data from Lawrence et al. (2012) (Fig. 2a). The PFTs included evergreen needleleaf tree (ENT), evergreen broadleaf tree (EBT), deciduous needleleaf tree

**Table 1** The information of observation sites for evaluating carbon allocation model

| Site name  | Lon      | Lat    | Plant functional types (dominant species)  | Treatment   | References           |
|------------|----------|--------|--|---|----------------------|
| Duke       | - 79.08  | 35.97  | Evergreen needleleaf tree, loblolly pine ( <i>Pinus taeda</i> ) plantation                           | The atmospheric $CO_2$ at elevated $CO_2$ and control sites from 1997 to 2005 are 542 and 342 ppmv  | De Kauwe et al. 2014 |
| Oak Ridge  | - 84.33  | 35.90  | Deciduous broadleaf tree, sweetgum ( <i>Liquidambar styraciflua</i> ) plantation                     | The atmospheric $CO_2$ at elevated $CO_2$ and control sites from 1999 to 2008 are 547 and 395 ppmv  | De Kauwe et al. 2014 |
| Caxiuana   | - 51.45  | - 1.72 | Evergreen broadleaf tree (undisturbed terra firme forest with more than 110 tree species $ha^{-1}$ ) | Approximately 50% of precipitation in the drought site was excluded from 2009 to 2011               | da Costa et al. 2014 |
| Oklahoma   | - 97.52  | 34.98  | C4 grass ( <i>Schizachyrium scoparium</i> and <i>Sorghastrum nutans</i> )                            | Air temperature was elevated by an average of $1.38^{\circ}C$ from 2005 to 2009 in the warming site | Xu et al. 2012       |
| Duolun     | 116.28   | 42.03  | C3 grass ( <i>Leymus chinensis</i> )   | //  | Xu et al. 2016       |
| Jornada    | - 106.85 | 32.60  | C4 grass ( <i>Bouteloua eriopoda</i> )   | //  | Hui and Jackson 2006 |
| Montecillo | - 98.91  | 19.46  | C4 grass ( <i>Distichlis spicata</i> )   | //  | Hui and Jackson 2006 |
| Matador    | - 102.72 | 50.70  | C3 grass ( <i>Agropyron</i> spp.)  | //  | Hui and Jackson 2006 |
| Tumugi     | 123.00   | 46.10  | C3 grass ( <i>Filifolium sibiricum</i> )   | //  | Hui and Jackson 2006 |

Lon longitude ("-" : Western Hemisphere), Lat latitude ("-" : Southern Hemisphere)



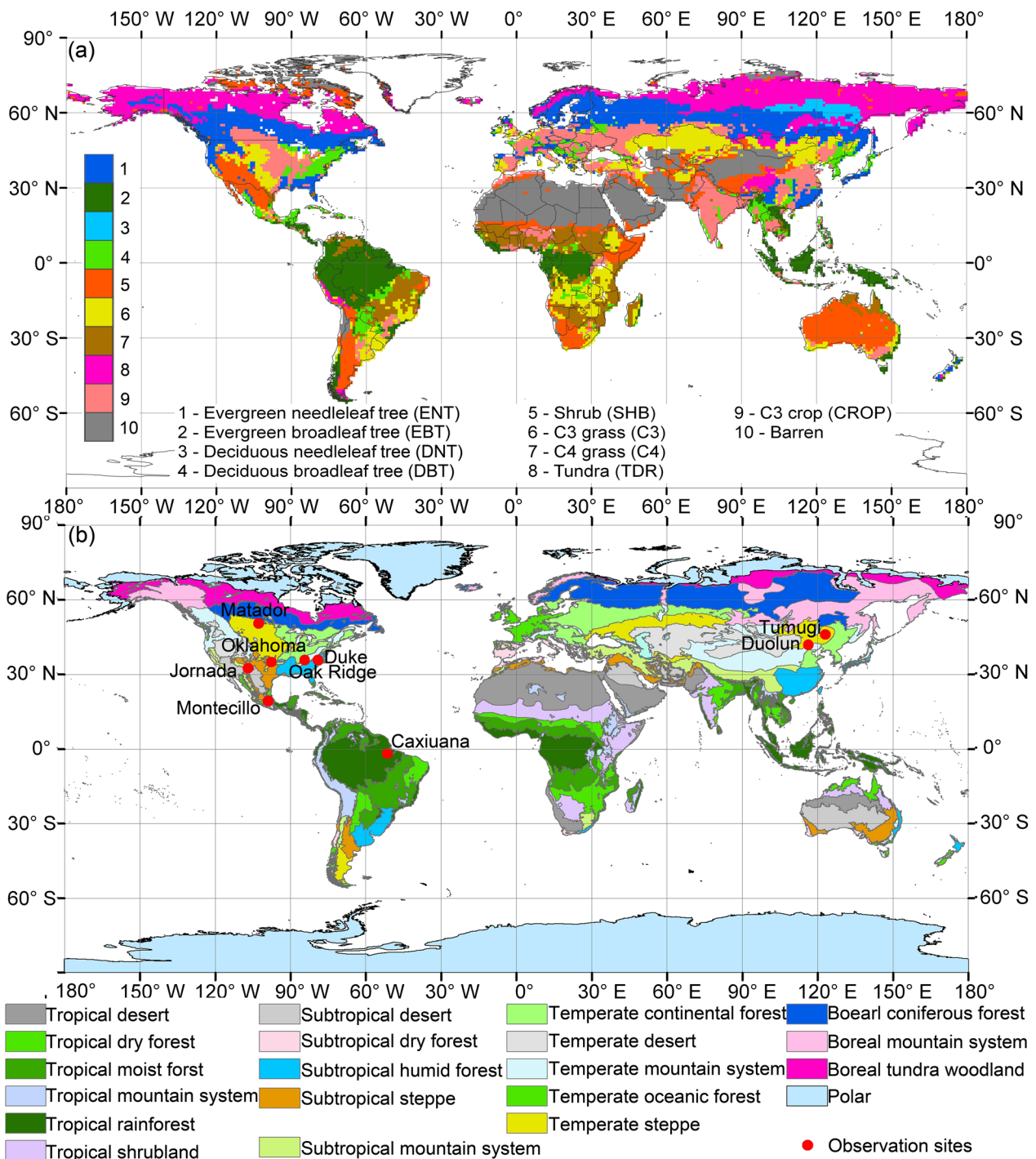


**Fig. 2** Global distribution of plant functional types in the CABLE model (a). The global ecological zones, and locations of the observation sites for carbon allocation (b)

(DNT), deciduous broadleaf tree (DBT), shrub (SHB), C3 grass (C3), C4 grass (C4), tundra (TDR), and C3 crop (CROP). The global ecological zone for forest reporting by the FAO was used to analyze the results (Fig. 2b, FAO 2012).

**Simulations**

To determine the influence of the four environmental variables, i.e., atmospheric CO<sub>2</sub> concentration, precipitation, air temperature, and incident shortwave radiation, on the spatiotemporal patterns of carbon allocation, we

performed five simulations (Table 2): (1) a control simulation, forced by the original MERRA climatic data and historical CO<sub>2</sub> observations from 1979 to 2014; (2) a CO<sub>2</sub>\_fixed simulation, forced by the original MERRA climatic data, with the atmospheric CO<sub>2</sub> concentration fixed at the 1979 level (337.0 ppm); and (3) Prec\_fixed, (4) Tair\_fixed and (5) Swd\_fixed simulations, forced by the data on the hourly precipitation, near surface air temperature and incident shortwave radiation of 1979 for all simulation years and historical CO<sub>2</sub> observations, respectively. We then quantified the effects of changes in each environmental variable at an inter-annual scale after 1979 on the carbon allocation by calculating the difference in ratios of carbon allocation between the control simulation and simulations in which the inter-annual variations of the given environmental variable after 1979 were not considered (e.g., Prec\_fixed simulation).

We conducted a spin-up run and two transient runs for the simulations. For the spin-up run, we ran the model 20 times by recycling the MERRA climatic datasets from 1979 to 2014. The atmospheric CO<sub>2</sub> concentration at the 1850 level (280.0 ppm) was used for this. Once the model had reached equilibrium state, it was run in the first transient mode (1850–1978) with varying CO<sub>2</sub> concentrations while recycling the MERRA climate datasets from 1979 to 2014. The second transient mode covered the period 1979–2014, and the corresponding CO<sub>2</sub> concentrations and climatic variables were used according to the design of the five simulations (Table 2).

## Results

### Effects of inter-annual changes in environmental variables on carbon allocation

The environmental variables significantly changed from 1979 to 2014 across the globe. Along with a rising atmospheric CO<sub>2</sub> concentration, the global mean surface temperature increased by 0.72 °C over 36 years (Fig. 3d). Moreover, the incident shortwave radiation and precipitation exhibited a trend of growth, with rates of increase of 0.12 W m<sup>-2</sup> yr<sup>-1</sup> and 2.27 mm yr<sup>-1</sup>, respectively (Fig. 3f, b). However, the climate variables were substantially spatially heterogeneous. Increased temperatures

were observed in all plant functional types. The largest increase in the temperature was observed in the tundra, 0.04 °C yr<sup>-1</sup> (Table 3), while the lowest increase in temperature increases were observed in evergreen broadleaf tree, at 0.009 °C yr<sup>-1</sup> (Table 3). On average, the precipitation showed a trend of decline from 1979 to 2014 only in the evergreen needleleaf tree and the deciduous needleleaf tree, while the largest increase in precipitation occurred in evergreen broadleaf tree (Table 3). Radiation exhibited a large spatial heterogeneity, and significant decreased in the evergreen broadleaf tree, shrub and C4 grass (Table 3).

Climate change significantly influenced resource availability. The global mean light availability showed a significantly decrease trend from 1979 to 2014 (Fig. 4a and Table 4). The model of carbon allocation in case of resource limitation showed that changes in light availability mainly depended on changes in the LAI. The largest decrease in light availability was caused by the greatest increase in the LAI as a result of the fertilization effect of CO<sub>2</sub> (Fig. 4a and d). Compared with the control simulation, the changes in air temperature increased the magnitude of global light availability (Fig. 4a and Table 4). The global precipitation exhibited a trend of an increase (Fig. 3b), and led to an increase in global water availability (i.e., soil moisture) from 1979 to 2014 (Fig. 4b and Table 4). Water availability exhibited the largest decrease in the Tair\_fixed simulation (Fig. 4b and Table 4), reflecting the dominant influence of the rising temperature on it. The global mean nitrogen availability showed a significant trend of increase from 1979 to 2014 as a result of the dominant influence of increasing precipitation (Fig. 4c and Table 4).

The effect of rising CO<sub>2</sub> levels on light availability was highly consistent across the globe. More than 83.54% of the global areas of land exhibited a significantly decreased light availability (Fig. 5a) as the LAI increased (Fig. 5d). Increased CO<sub>2</sub> concentrations led to an increase in water availability in 63.46% of the global areas of land (Fig. 5b), which in turn controlled the pattern of nitrogen availability except in the northern Amazon (Fig. 5c). Increased CO<sub>2</sub> resulted in decreased soil moisture in semi-arid and arid ecological zones (Figs. 2b and 5b). The simulations of the change in precipitation showed that the change in the moisture content of soil, nitrogen availability, and the LAI showed similar patterns to that of the trend of precipitation (Figs. 3a, 5f, g, and h). Thus, light availability exhibited the opposite pattern of change to that of precipitation (Figs. 3a and 5e).

Compared with those of the atmospheric CO<sub>2</sub> and precipitation, the effects of the temperature and shortwave radiation on the availability of resources and the LAI were more complicated (Fig. 6). Increased temperature led to a

**Table 2** Design of simulations of the CABLE model

| ID | Experiment             | Climate                          | CO <sub>2</sub>              |
|----|------------------------|----------------------------------|------------------------------|
| 1  | Control                | 1979–2014                        | 1979–2014                    |
| 2  | CO <sub>2</sub> _fixed | 1979–2014                        | Fixed CO <sub>2</sub> (1979) |
| 3  | Prec_fixed             | Fixed precipitation (1979)       | 1979–2014                    |
| 4  | Tair_fixed             | Fixed temperature (1979)         | 1979–2014                    |
| 5  | Swd_fixed              | Fixed shortwave radiation (1979) | 1979–2014                    |

CO<sub>2</sub> atmospheric CO<sub>2</sub> concentration; Prec precipitation; Tair air temperature; and Swd incident shortwave radiation

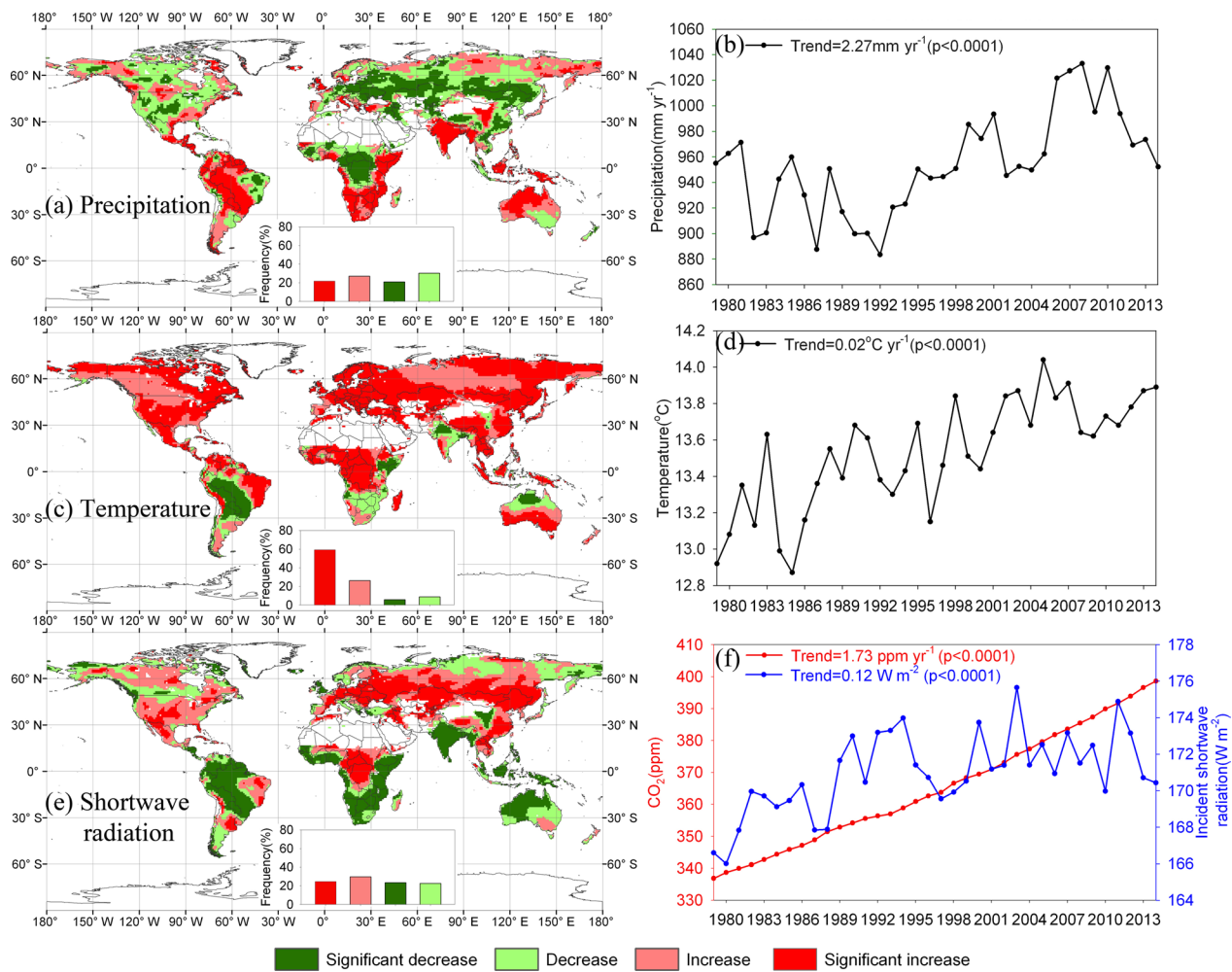


**Fig. 3** The trends and inter-annual variations of the global mean precipitation (a, b), air temperature (c, d), incident shortwave radiation (e, f) and atmospheric CO<sub>2</sub> concentration (f) from 1979 to 2014

decrease in the availability of water in soil in 70.97% of the global area of land (Fig. 6b) and increased nitrogen availability at high northern latitudes (60° N to 90° N, Fig. 6c). The decrease in the LAI in the Congo rainforest due to warming was consistent with the decrease in water availability in this region (Figs. 3c, 6b, and d). The effects of shortwave radiation on water availability exhibited the opposite pattern to that of the shortwave radiation (Figs. 3e and 6f). In the Northern Hemisphere, the effect of the shortwave radiation on the LAI was consistent with its own trend (Figs. 3e and 6h), while the increase in the LAI was consistent with that in water availability caused by the change in the shortwave radiation in the Southern Hemisphere (Figs. 3e, 6f, and h).

### Effects of climate change on carbon allocation

Global climate change has led to substantial changes in carbon allocation among the three parts of plants, i.e., roots, leaves, and wood tissues. The carbon allocation to the leaves (aleaf) and wood (awood) significantly increased from 1979 to 2014 (Fig. 7a, b, and Table 5), while its allocation to roots (aroot) decreased in this period (Fig. 7c and Table 5). However, the climatic variables had different effects on the changes in carbon allocation. The allocation to leaves was significantly reduced by rising atmospheric CO<sub>2</sub> concentration (Fig. 7a and Table 5). By contrast, the changes in precipitation and shortwave radiation enhanced the global mean carbon allocation to the leaves (Fig. 7a and Table 5). The rising

**Table 3** Magnitudes and trends of the environmental variables from 1979 to 2014 in regions with different plant functional types (PFTs)

| PFTs (area percentage, unit:%) | Magnitude             |                             |           |                          | Trend                                   |                             |                             |   |
|--------------------------------|-----------------------|-----------------------------|-----------|--------------------------|---|-----------------------------|-----------------------------|---|
|                                | CO <sub>2</sub> (ppm) | Prec (mm yr <sup>-1</sup> ) | Tair (°C) | Swd (W m <sup>-2</sup> ) | CO <sub>2</sub> (ppm yr <sup>-1</sup> ) | Prec (mm yr <sup>-1</sup> ) | Tair (°C yr <sup>-1</sup> ) | Swd (W m <sup>-2</sup> yr <sup>-1</sup> ) |
| ENT (13.4)                     | 365.26                | 824.6                       | 2.8       | 147.73                   | 1.73**                                  | -1.48**                     | 0.03**                      | 0.094**                                   |
| EBT (13.1)                     |                       | 2304.5                      | 23.7      | 213.2                    |   | 10.88**                     | 0.009                       | -0.34**                                   |
| DNT (0.9)                      |                       | 423.65                      | -8.2      | 122.28                   |   | -0.74                       | 0.039*                      | 0.085*                                    |
| DBT (6.4)                      |                       | 1207.8                      | 18.16     | 209.33                   |   | 2.20**                      | 0.012**                     | 0.00                                      |
| SHB (15.9)                     |                       | 415.62                      | 17.51     | 247.12                   |   | 2.48**                      | 0.02**                      | -0.09**                                   |
| C3 (13.1)                      |                       | 667.86                      | 14.07     | 217.67                   |   | 0.26                        | 0.03**                      | 0.01                                      |
| C4 (10.8)                      |                       | 1042.6                      | 26.43     | 240.63                   |   | 2.32                        | 0.02**                      | -0.13**                                   |
| TDR (12.2)                     |                       | 559.65                      | -6.51     | 124.7                    |   | 0.11                        | 0.04**                      | 0.00                                      |
| CROP (14.2)                    |                       | 881.03                      | 15.92     | 197.13                   |   | 1.49**                      | 0.02**                      | -0.02                                     |

CO<sub>2</sub> atmospheric CO<sub>2</sub> concentration; Prec precipitation; Tair air temperature; Swd incident shortwave radiation; ENT evergreen needleleaf tree; EBT evergreen broadleaf tree; DNT deciduous needleleaf tree; DBT deciduous broadleaf tree; SHB shrub; C3 C3 grass; C4 C4 grass; TDR tundra; CROP C3 crop

\*\* Highly significant change ( $p < 0.01$ )

\* Significant change ( $p < 0.05$ )

atmospheric CO<sub>2</sub> and precipitation led to significant increases in awood (Fig. 7b and Table 5), but it significantly decreased with increasing temperature (Fig. 7b and Table 5). The rising precipitation contributed to the largest decrease in aroot (Fig. 7c and Table 5).

At the regional scale, the rising atmospheric CO<sub>2</sub> concentration increased awood to over 80% in woody plants (Fig. 8b). The allocation to leaves decreased with increasing CO<sub>2</sub> concentration in the wooden biomes, except at high northern latitudes (60° N to 90° N) and in Australia (Fig. 8a), while aroot exhibited a widespread decrease (Fig. 8c). In response to rising atmospheric CO<sub>2</sub> concentration, aroot consistently increased and aleaf consistently decreased in grasslands (Figs. 2, 8a, and c). Increased precipitation enhanced the values of awood (Figs. 8e and 3a), while it led to the largest increase in values of awood in shrubs (Fig. 8e). By contrast, aroot decreased with increasing precipitation (Figs. 8f and 3a). The response of aleaf to precipitation was complicated. For example, it increased with the increasing precipitation in Australia but increased with decreasing precipitation in the Congo Basin (Figs. 8d and 3a). The responses of the ratios of carbon allocation to the temperature were more complicated than those to the CO<sub>2</sub> concentration

and precipitation because of the divergent influence of the temperature on nitrogen availability (Figs. 8g, h, i, and 6c).

## Discussion

The CABLE model was able to accurately simulate the processes of response of resource availability and carbon allocation to environmental changes. Elevated air temperature at the C4 grass site in Oklahoma increased the temperature of soil and reduced the availability of water in it, resulting in more carbon being allocated to the roots to efficiently capture water (McCarthy and Enquist 2007; Xu et al. 2012). A reduction in the rainfall reduced the availability of water in soil while increasing aroot and reducing awood at the Caxiuana site (da Costa et al. 2014). The CABLE model also correctly simulated the decreased availability of water in soil and increased aroot under warming and drought conditions (Xia et al. 2017). At the Duke site, the increase in CO<sub>2</sub> concentration enhanced the soil moisture by reducing stomatal conductance and transpiration per unit area of the leaf, and reduced light availability by stimulating leaf growth (McCarthy et al. 2010; Ward et al. 2013; De Kauwe et al. 2014). Both of these effects stimulated the values of

(See figure on next page.)

**Fig. 4** Inter-annual variations in the global mean availability of light (a), water (b), and nitrogen (c), and leaf area index (LAI, d) in the control simulation (right vertical axis and the red line). Differences in the four variables between the control simulation, and the fixed CO<sub>2</sub> (CO<sub>2</sub>\_fixed), fixed precipitation (Prec\_fixed), fixed temperature (Tair\_fixed), and fixed shortwave radiation (Swd\_fixed) simulations (left vertical axis). For example, "Light\_Control-Light\_CO<sub>2</sub>\_fixed" refers to the difference in light availability between the control and the CO<sub>2</sub>\_fixed simulations, and negative values indicate that changes in CO<sub>2</sub> led to a decrease in light availability



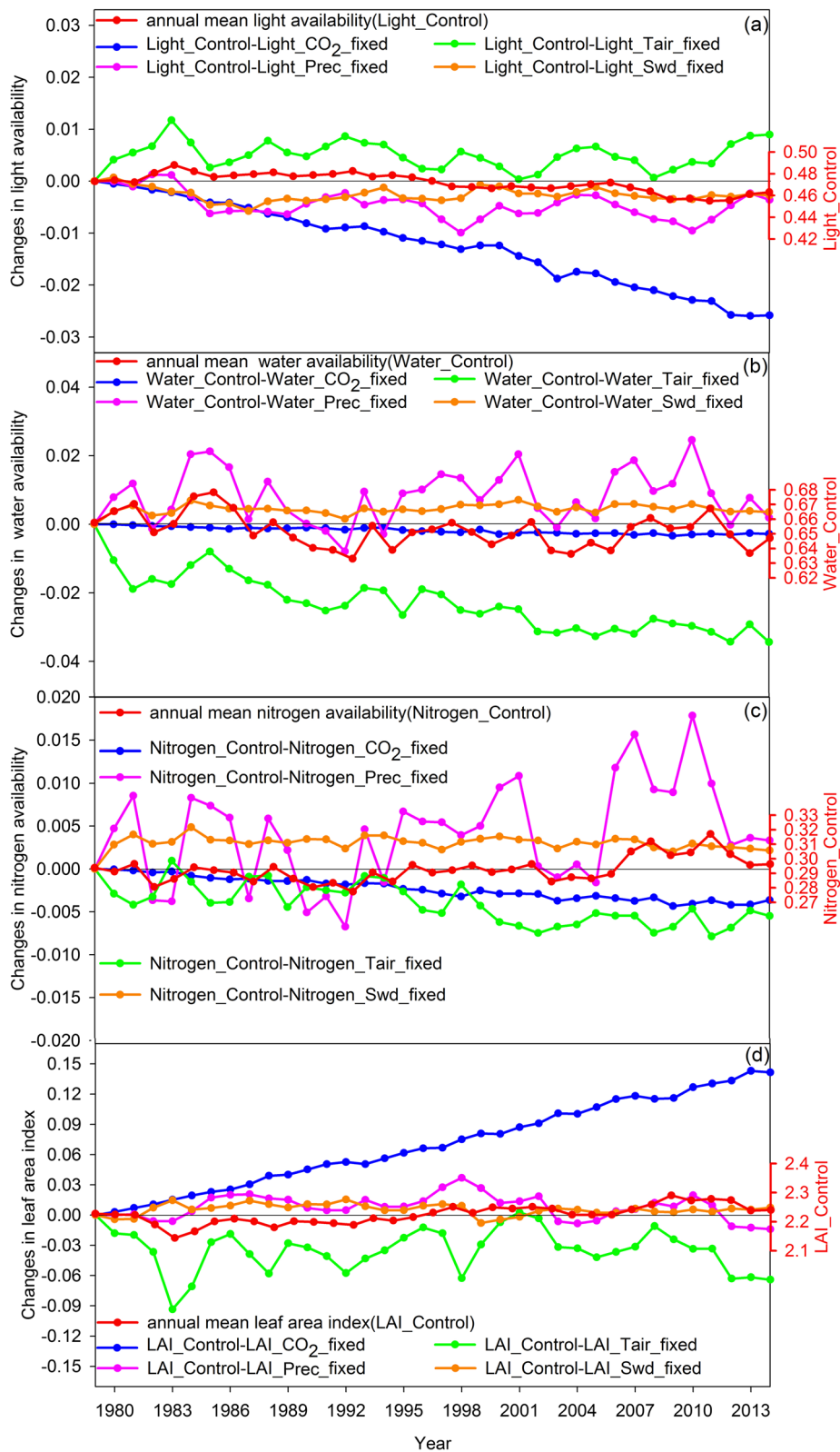


**Fig. 4** (See legend on previous page.)



**Table 4** Magnitudes and trends of the global mean availability of light, water, and nitrogen from 1979 to 2014 in the control simulation

| Simulations                    | Magnitude                     |                              |                               | Trend                |                       |                     |
|--------------------------------|-------------------------------|------------------------------|-------------------------------|----------------------|-----------------------|---------------------|
|                                | Light                         | Water                        | Nitrogen                      | Light                | Water                 | Nitrogen            |
| Control                        | 0.471 ± 0.009 <sup>a</sup>    | 0.652 ± 0.012 <sup>ab</sup>  | 0.293 ± 0.009 <sup>a</sup>    | - 0.001 <sup>*</sup> | - 4.0E-4 <sup>*</sup> | 4.0E-4 <sup>*</sup> |
| Control-CO <sub>2</sub> _fixed | - 0.012 ± 0.008 <sup>b</sup>  | - 0.002 ± 0.001 <sup>a</sup> | - 0.002 ± 0.001 <sup>ab</sup> | - 7.8E-4             | 0.0                   | - 1.0E-4            |
| Control-Prec_fixed             | - 0.004 ± 0.003 <sup>c</sup>  | 0.008 ± 0.008 <sup>b</sup>   | 0.004 ± 0.006 <sup>c</sup>    | - 2.0E-4             | 1.0E-4                | 2.0E-4              |
| Control-Tair_fixed             | 0.005 ± 0.003 <sup>d</sup>    | - 0.023 ± 0.008 <sup>c</sup> | - 0.004 ± 0.002 <sup>b</sup>  | - 1.0E-4             | - 6.0E-4              | - 2.0E-4            |
| Control-Swd_fixed              | - 0.003 ± 0.001 <sup>ac</sup> | 0.004 ± 0.001 <sup>b</sup>   | 0.003 ± 0.001 <sup>a</sup>    | - 1.0E-4             | 1.0E-4                | 0.0                 |

Trends of differences in the availability of light, water, and nitrogen between the control simulation, and the fixed CO<sub>2</sub> (CO<sub>2</sub>\_fixed), fixed precipitation (Prec\_fixed), fixed temperature (Tair\_fixed), and fixed shortwave radiation (Swd\_fixed) simulations. The letters indicate the statistical significance of ratios of carbon allocation in the five simulations ( $p < 0.05$ )

CO<sub>2</sub> atmospheric CO<sub>2</sub> concentration; Prec precipitation; Tair air temperature; and Swd incident shortwave radiation

\* indicates a statistically significant level ( $p < 0.05$ )

awood. The CABLE model was able to accurately represent the effects of eCO<sub>2</sub> on the LAI, light and water availability, and carbon allocation (Xia et al. 2017). The increase in aroot at the Oak Ridge site might have been caused by a reduction in the availability of nitrogen in soil (Norby et al. 2010). The CABLE model could not completely reproduce the changes in carbon allocation at this site partly because of the complicated effects of eCO<sub>2</sub> on this deciduous forest ecosystem.

The rising atmospheric CO<sub>2</sub> concentration enhanced the LAI over most areas of the globe (Fig. 5d). It ultimately influenced carbon allocation by altering the LAI, which is an important property of the ecosystem that determines the surface temperature and soil water balance (Luyssaert et al. 2014; Shen et al. 2015). Rising CO<sub>2</sub> concentrations stimulated photosynthesis, which increased the LAI (Zhu et al. 2016). Our simulations showed larger increases in the LAI over low latitudes (Fig. 5d), which is consistent with the results of previous studies (Zhu et al. 2016). The enhanced LAI reduced light availability according to the self-shading rule, but had a weak effect on the availability of water and nitrogen (Table 4). Consequently, changes in these resources enhanced the allocation of carbon to wooden parts of plants and benefited the carbon storage of terrestrial ecosystems (Ise et al. 2010; Poorter et al. 2012).

The effects of eCO<sub>2</sub> on water availability were controlled by two processes in the CABLE model: (1) eCO<sub>2</sub> decreased the stomatal conductance and transpiration, which led to an increase in the soil moisture. (2) The increased LAI enhanced transpiration and reduced the soil moisture. The results of this study as well as previous ones support the mechanism of response of water availability to the eCO<sub>2</sub> as represented by the CABLE model (De Kauwe et al. 2013; Cheng et al. 2014). The

decrease in the soil moisture in water-limited PFTs (i.e., shrubs and C3 grass) was caused by the increase in the LAI (Figs. 2, 5b, and d), where this is consistent with the study by Donohue et al. (2009). The C3 grass allocated more carbon to roots under water stress condition (Fig. 8c). With regard to the other PFTs, an increase in CO<sub>2</sub> concentration mostly led to an increase in the soil moisture (Fig. 5b). The decrease in carbon allocation to the roots in boreal evergreen needleleaf tree in particular was determined by the increase in the availability of water in soil (Figs. 2, 5b, and 8c).

The effects of precipitation on carbon allocation were substantially spatially heterogeneous owing to inhomogeneous changes in the precipitation and the responses of the ecosystem. Decreased precipitation was found in the most areas of the Northern Hemisphere, and restricted the growth of vegetation and reduced the LAI. However, the decreased precipitation increased soil temperature in the high latitude regions of the Northern Hemisphere (Figs. 3a and 9b) and stimulated vegetation growth (Yuan et al. 2014). Moreover, the increased precipitation in the Amazon rainforest did not enhance the LAI, but resulted in a slight decrease in it instead (Figs. 3a and 5h). One potential cause of this was the reduced radiation with increased precipitation (Myneni et al. 2007). Precipitation dominated the changes in soil moisture as well as nitrogen availability according to the CABLE model (Fig. 5f and g). In general, decreased precipitation reduced the soil moisture and the LAI, and increased the availability of light, while changes in both the soil moisture and light enhanced carbon allocation to the roots but restricted that to the wooden parts and leaves of plants (Waring 1991; Poorter et al. 2012; Perrin and Mitchell 2013).

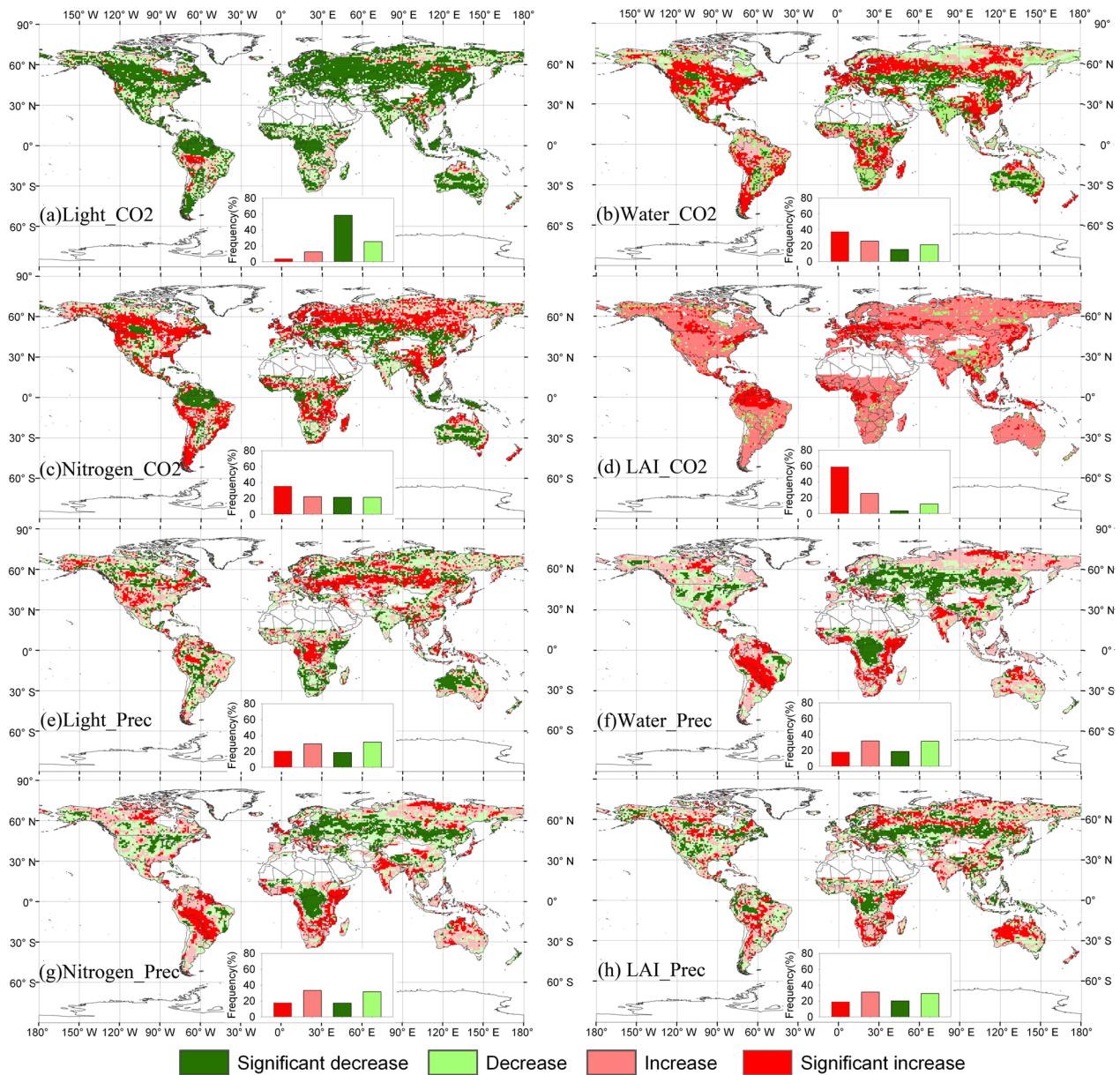


**Fig. 5** Trends of the differences in the availability of light (a), water (b), and nitrogen (c) as well as the leaf area index (LAI, d) between the control simulation and the fixed CO<sub>2</sub> (i.e., CO<sub>2</sub>\_fixed in Table 2) simulation. Trends of differences in the availability of light (e), water (f), and nitrogen (g) as well as the leaf area index (LAI, h) between the control simulation and the fixed precipitation (i.e., Prec\_fixed in Table 2) simulation

The effects of the temperature and shortwave radiation on carbon allocation are mainly accomplished by influencing the soil moisture and LAI in the CABLE model. Warming increased evaporation and reduced the soil moisture (Figs. 3c, 3e, 6b, and f), where this outcomes is consistent with that reported in previous studies (Xu et al. 2013; Samaniego et al. 2018). The reduced soil moisture led to increased carbon allocation to the roots of plants (Fig. 8i). Warming resulted in an increased LAI in most regions with boreal evergreen needleleaf tree

and the tundra (Figs. 2 and 6d), where this is consistent with findings based on remote sensing observations (Piao et al. 2020). This process increased the allocation of carbon to wood tissues in the relevant PFTs (Fig. 8h).

The responses of carbon allocation to climate change were influenced by several uncertainties in the former in the CABLE model. Empirical equations for the availability of nitrogen led to uncertainties in the dynamics of the response of nitrogen in the soil to climate change and its effects on carbon allocation. This empirical equation

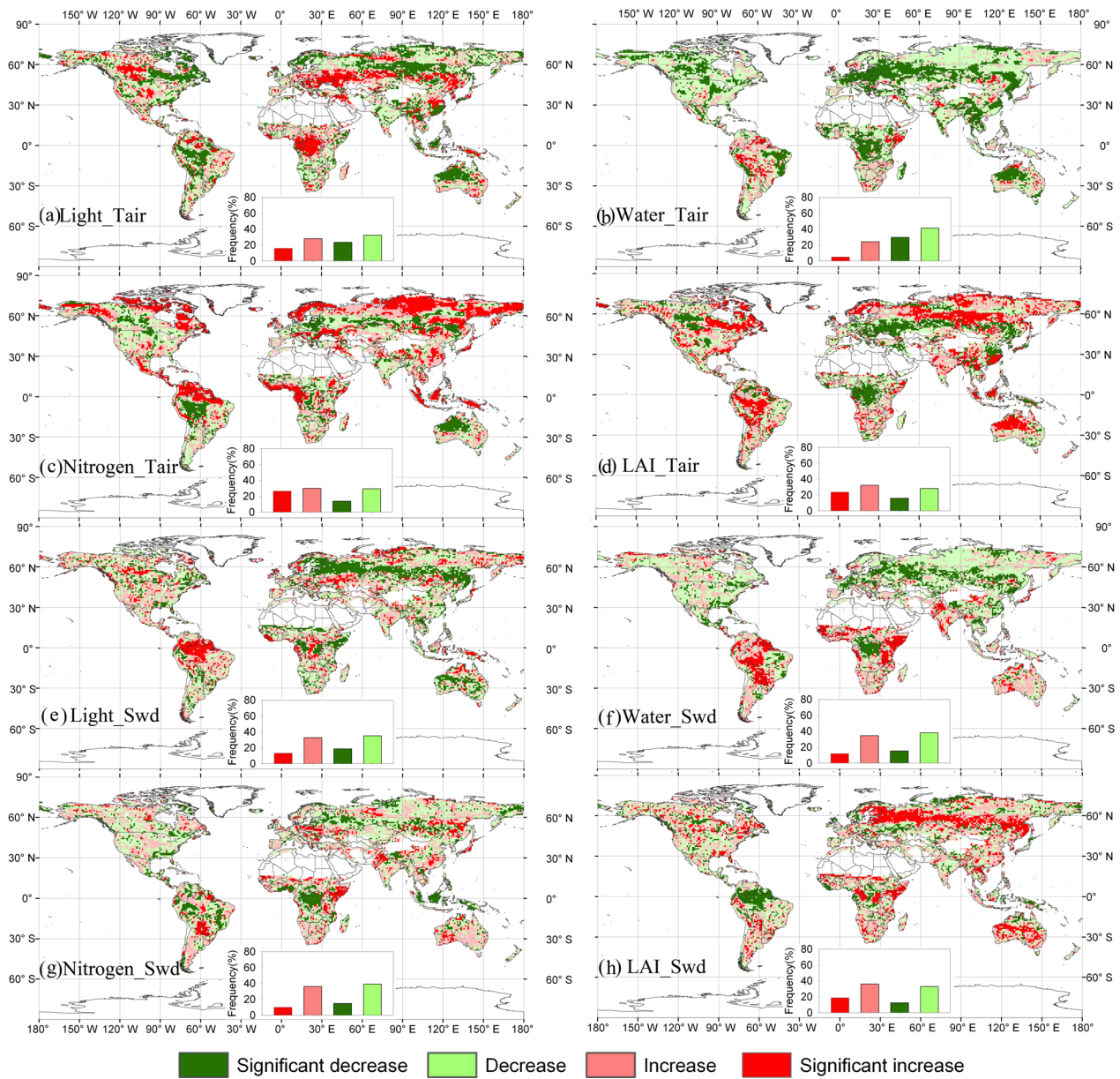


**Fig. 6** Trends of the differences in the availability of light (a), water (b), and nitrogen (c) as well as the leaf area index (LAI, d) between the control simulation and the fixed temperature (i.e., Tair\_fixed in Table 2) simulation. Trends of differences in the availability of light (e), water (f), and nitrogen (g), and the leaf area index (LAI, h) between the control simulation and the fixed incident shortwave radiation (i.e., Swd\_fixed in Table 2) simulation

assumed that spatial variability in the mineralization of nitrogen and the decomposition of the organic matter in soil were identical (Townsend et al. 1995). The availability of nitrogen is calculated as the product of the abiotic factors of the temperature and moisture (Potter et al. 1993). The abiotic factor of the temperature has a standard  $Q_{10}$  formulation, while the availability of nitrogen increases with the temperature. However, the simulations on warming suggested that elevated temperature tended to increase the net nitrogen mineralization in the first year

but reduced decrease it in the subsequent years, a process that is attributable to stimulated plant growth and belowground carbon allocation that enhanced the immobilization of microbial nitrogen (Wan et al. 2004). Moreover, the soil moisture strongly regulated the aerobic and anaerobic conditions, which determined the magnitude of nitrification and denitrification as well as the availability of nitrogen (Xu and Prentice 2008). However, the effects of soil moisture on the availability of nitrogen were largely spatially heterogeneous.



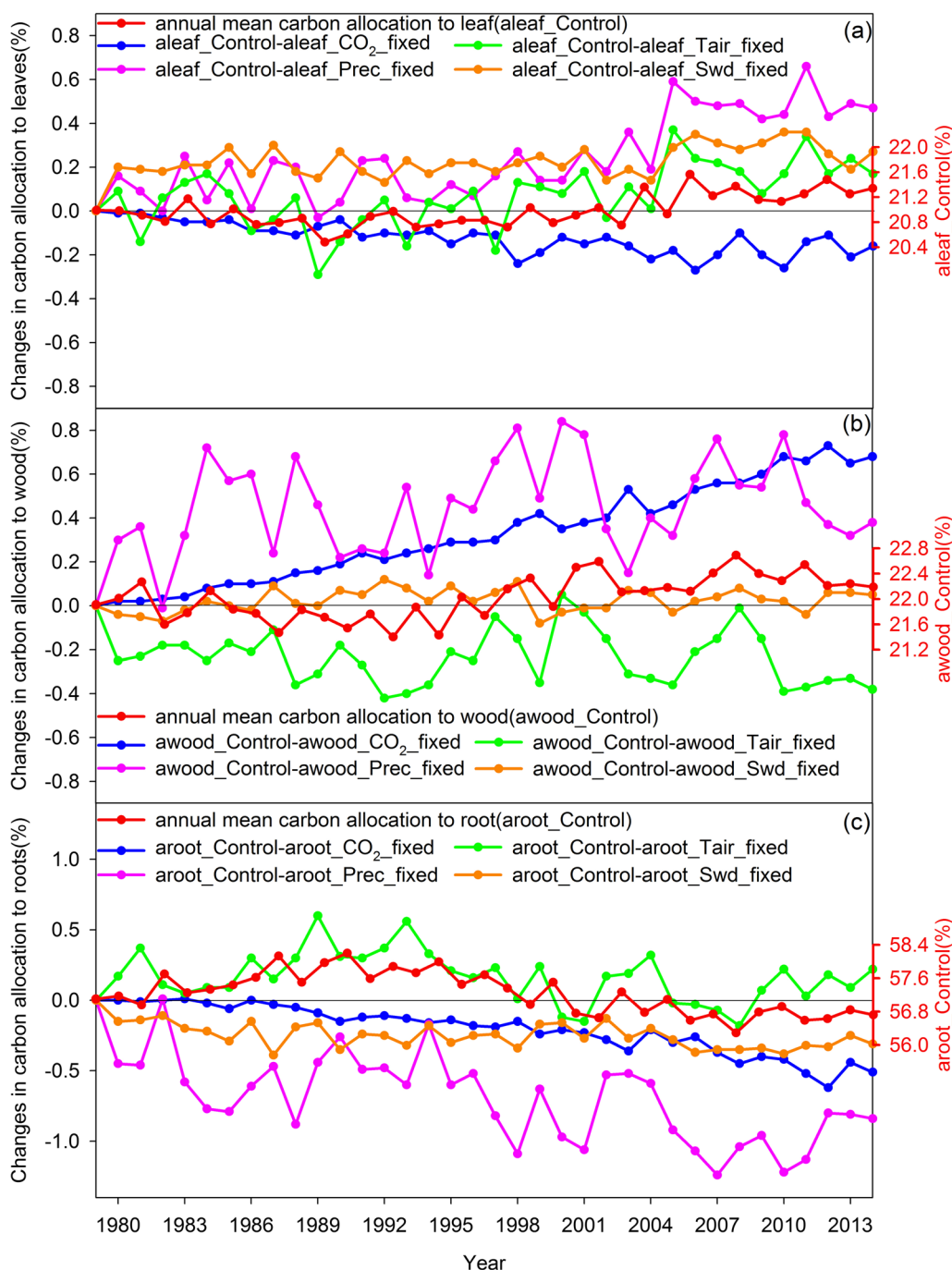


**Fig. 7** Inter-annual variations in the global mean carbon allocation to the leaves (aleaf, **a**), wood (awood, **b**), and roots (aroot, **c**) of plants in the control simulation (right vertical axis and red line). Differences in the ratios of carbon allocation between the control simulation, and the fixed CO<sub>2</sub> (CO<sub>2</sub>\_fixed), fixed precipitation (Prec\_fixed), fixed temperature (Tair\_fixed), and fixed shortwave radiation (Swd\_fixed) simulations (left vertical axis). For example, "aleaf\_Control-aleaf\_CO<sub>2</sub>\_fixed" refers to the difference in values of aleaf between the control and the CO<sub>2</sub>\_fixed simulations, while negative values mean that the changes in CO<sub>2</sub> concentration led to decrease in aleaf. CO<sub>2</sub> atmospheric CO<sub>2</sub> concentration; Prec precipitation; Tair air temperature; Swd incident shortwave radiation

Moreover, light condition is one of the most important environmental factors influencing carbon allocation (Iszkuła and Boratyński 2004, 2006). However, the

availability of light was not calculated from downwelling radiation, but from leaf area index because the plant at the lower canopy might have had increased access to

**Table 5** Magnitudes and trends of the global mean carbon allocation to the leaves (aleaf), wood (awood), and roots (aroot) of plants from 1979 to 2014 according to the control simulation

| Simulations                    | Magnitude                 |                           |                            | Trend                |                      |                       |
|--------------------------------|---------------------------|---------------------------|----------------------------|----------------------|----------------------|-----------------------|
|                                | aleaf (%)                 | awood (%)                 | aroot (%)                  | aleaf (%)            | awood (%)            | aroot (%)             |
| Control                        | 20.99 ± 0.25 <sup>a</sup> | 22.04 ± 0.34 <sup>a</sup> | 56.98 ± 0.52 <sup>a</sup>  | 0.0146 <sup>**</sup> | 0.0195 <sup>**</sup> | -0.0341 <sup>**</sup> |
| Control-CO <sub>2</sub> _fixed | -0.12 ± 0.07 <sup>b</sup> | 0.33 ± 0.22 <sup>b</sup>  | -0.21 ± 0.17 <sup>ab</sup> | -0.0053              | 0.0209               | -0.0156               |
| Control-Prec_fixed             | 0.24 ± 0.19 <sup>c</sup>  | 0.45 ± 0.22 <sup>b</sup>  | -0.69 ± 0.32 <sup>c</sup>  | 0.014                | 0.0062               | -0.0202               |
| Control-Tair_fixed             | 0.07 ± 0.14 <sup>a</sup>  | -0.23 ± 0.13 <sup>c</sup> | 0.16 ± 0.18 <sup>a</sup>   | 0.0076               | -0.0024              | -0.0052               |
| Control-Swd_fixed              | 0.22 ± 0.07 <sup>c</sup>  | 0.02 ± 0.05 <sup>a</sup>  | -0.25 ± 0.09 <sup>b</sup>  | 0.0037               | 0.0013               | -0.005                |

The magnitudes and trends of the differences in carbon allocation to the leaves (aleaf), wood (awood), and roots (aroot) between the control simulation, and the fixed CO<sub>2</sub> (CO<sub>2</sub>\_fixed), fixed precipitation (Prec\_fixed), fixed temperature (Tair\_fixed), and fixed shortwave radiation (Swd\_fixed) simulations. The letters indicate statistical significance of the ratios of carbon allocation in the five simulations ( $p < 0.05$ )

CO<sub>2</sub> atmospheric CO<sub>2</sub> concentration; *Prec* precipitation; *Tair* air temperature; and *Swd* incident shortwave radiation

<sup>\*\*</sup> Highly significant change ( $p < 0.01$ )

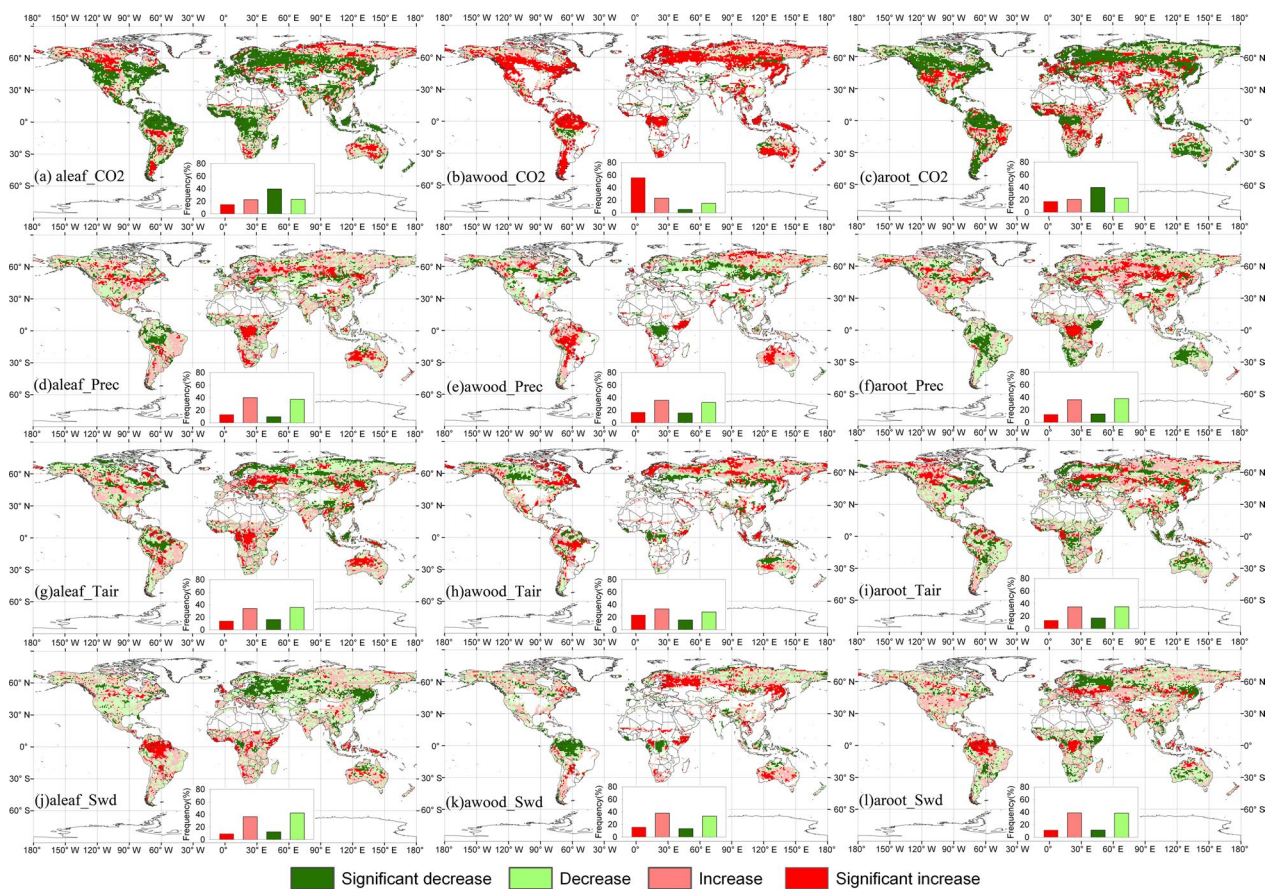


**Fig. 8** Trends of the differences in carbon allocation to the leaves (aleaf), wood (awood), and roots (aroot) between the control simulation, and fixed CO<sub>2</sub> (CO<sub>2</sub>\_fixed), fixed precipitation (Prec\_fixed), fixed temperature (Tair\_fixed), and fixed shortwave radiation (Swd\_fixed) simulations. For example, "aleaf\_CO<sub>2</sub>" refers to the difference in carbon allocation to leaves between the control and the CO<sub>2</sub>\_fixed simulations. CO<sub>2</sub> atmospheric CO<sub>2</sub> concentration; *Prec* precipitation; *Tair* air temperature; *Swd* incident shortwave radiation



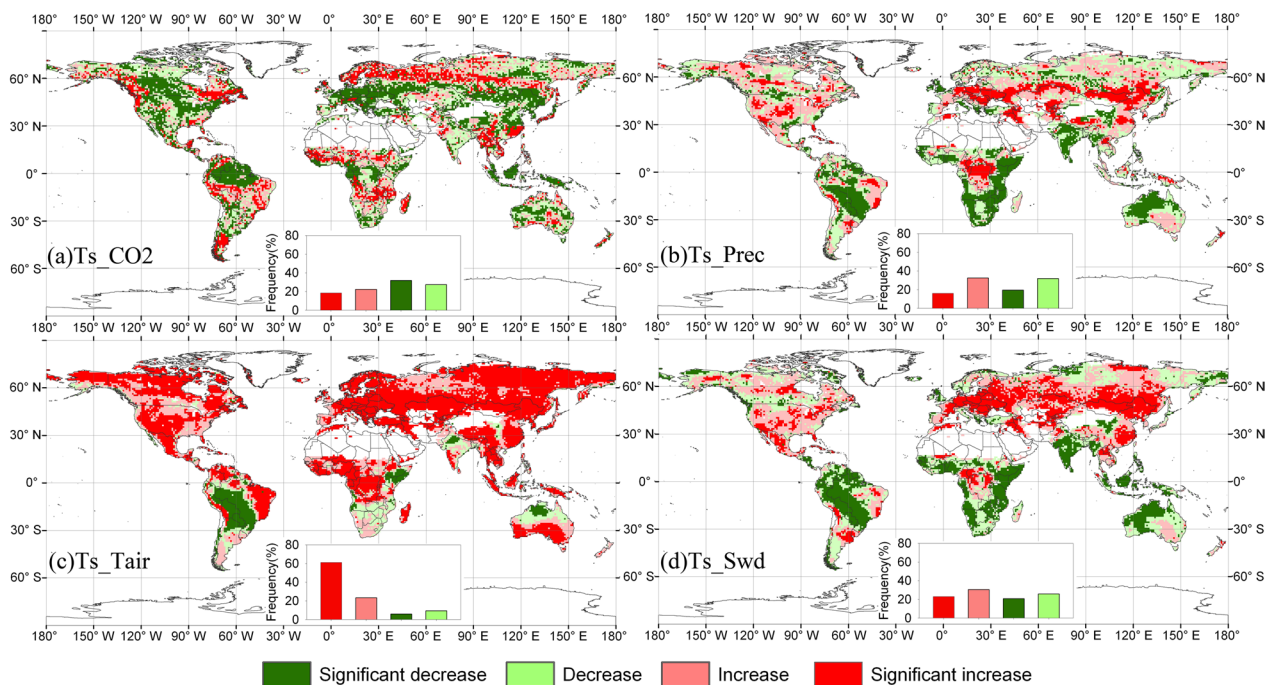


**Fig. 9** Differences in the temperature limitation factor [Ts, see Eq. (9)] in the availability of nitrogen between the control simulation, and the simulations in which certain climatic variables were kept constant. For example, “Ts\_CO<sub>2</sub>” refers to the difference in the temperature limitation factor between the control simulation, and the CO<sub>2</sub>-fixed simulation. CO<sub>2</sub> atmospheric CO<sub>2</sub> concentration; *Prec* precipitation; *Tair* air temperature; *Swd* incident shortwave radiation

light through increased allocation of carbon to the stem (Friedlingstein et al. 1999). This method has been used in several models, including Canadian terrestrial ecosystem model (CTEM; Arora and Boer 2005), organizing carbon and hydrology in dynamic Ecosystems (ORCHIDEE; Krinner et al. 2005), and adaptive dynamic global vegetation model (aDGVM; Scheiter and Higgins 2009). Numerous experiments have shown that plants allocate a higher fraction of carbon to stems and leaves under a low incident radiation above the canopy (Poorter et al. 2012). For example, compared with plants grown at higher irradiance, shaded plants generally have a higher specific leaf area (SLA), and allocate more biomass to the leaves than to the roots for the efficient capture of light (Poorter 1999; Franck et al. 2007; Feng and Li 2007). The effect of downwelling radiation on the carbon allocation to the leaves should be considered in the terrestrial ecosystem model (Chen et al. 2020).

### Conclusions

In this study, we used the global land-surface model CABLE to investigate the contributions of changes in atmospheric CO<sub>2</sub> concentration, precipitation, air temperature, and incident shortwave radiation to global carbon allocation from 1979 to 2014. The model showed that rising atmospheric CO<sub>2</sub> concentration had reduced

the availability of light and increased that of water at a global scale, where this had enhanced carbon allocation to the wood tissues of plants. By contrast, the global mean precipitation exhibited an increasing trend, leading to an increase in the availability of water and a decrease in that of light. This had led to a reduction in carbon allocation to the roots and an increase in allocation to the wooden parts of plants. Rising atmospheric CO<sub>2</sub> concentration had led to a uniform increase in carbon allocation to wooden parts of the plants as well. However, the responses of the ratios of carbon allocation to temperature exhibited a large spatial heterogeneity, and were more complicated than those of the CO<sub>2</sub> concentration and precipitation because of the opposite effects of air temperature to the soil temperature and moisture. Although the observations of four manipulation experiments show that the CABLE model can accurately reflect the response mechanism of resource availability and carbon allocation to environmental change, there is still uncertainty in the inference of carbon allocation for different plant functional groups at the global scale. More studies are needed to model and verify the responses of carbon allocation by plants to multiple environmental changes based on models and field experiments in the future.

**Abbreviations**

|                  |  |
|------------------|--|
| CABLE            | Community Atmosphere Biosphere Land Exchange                             |
| NPP              | Net primary productivity   |
| CASA-CNP         | CASA (Carnegie–Ames–Stanford Approach)–CNP (carbon–nitrogen–phosphorous) |
| VISIT            | Vegetation Integrative Simulator for Trace gases                         |
| eCO <sub>2</sub> | Elevated atmospheric CO <sub>2</sub>                                     |
| aleaf            | Allocation coefficients for leaves                                       |
| awood            | Allocation coefficients for woody tissues                                |
| aroot            | Allocation coefficients for roots  |
| L                | Light availability   |
| W                | Water availability   |
| N                | Nitrogen availability  |
| MERRA            | Modern-Era Retrospective analysis for Research and Applications          |
| Tai              | Air temperature  |
| Prec             | Precipitation  |
| Swd              | Incident shortwave radiation   |
| Lwd              | Incident longwave radiation  |
| Qair             | Specific humidity  |
| Wind             | Wind speed   |
| Ps               | Pressure   |
| PFTs             | Plant functional types   |
| ENT              | Evergreen needleleaf tree  |
| DNT              | Deciduous needleleaf tree  |
| EBT              | Evergreen broadleaf tree   |
| DBT              | Deciduous broadleaf tree   |
| SHB              | Shrub  |
| C3               | C3 grass   |
| C4               | C4 grass   |
| TDR              | Tundra   |
| CROP             | C3 crop  |
| LAI              | Leaf area index  |
| CTEM             | Canadian Terrestrial Ecosystem Model                                     |
| ORCHIDEE         | Organizing Carbon and Hydrology in Dynamic Ecosystems                    |
| aDGM             | Adaptive Dynamic Global Vegetation Model                                 |
| SLA              | Specific leaf area   |

**Acknowledgements**

The MERRA data used here are downloaded at <http://disc.sci.gsfc.nasa.gov/daac-bin/FTPSubset.pl>. The global ecological zones (GEZ) for FAO forest reporting can be downloaded at <https://data.apps.fao.org/map/catalog/static/api/records/2fb209d0-fd34-4e5e-a3d8-a13c241eb61b>.

**Author contributions**

WY and JX conceived the research. WY supervised the research. JX and YC conducted the model runs. JX and YC conducted the data analysis. JX and WY drafted the manuscript. All authors contributed to the writing of the manuscript. All authors read and approved the final manuscript.

**Funding**

This study was supported by grants from the National Natural Science Foundation of China (Grant No. 42001094), Scientific Research Project of Tianjin Municipal Education Commission, China (Grant No. 2020KJ002) and Natural Science Foundation of Tianjin, China (Grant No. 18JCQNJC78100).

**Availability of data and materials**

The data sets used in the current study are available from the corresponding author on reasonable request.

**Declarations****Ethics approval and consent to participate**

Not applicable.

**Consent for publication**

Not applicable.

**Competing interests**

The authors declare that they have no competing interests.

Received: 1 July 2023 Accepted: 8 December 2023

Published online: 18 December 2023

**References**

- Aber JD, Melillo JM (1991) Terrestrial ecosystems. Saunders, Philadelphia, Pennsylvania, USA
- Arora VK, Boer GJ (2005) A parameterization of leaf phenology for the terrestrial ecosystem component of climate models. *Global Change Biol* 11(1):39–59
- Bird JA, Torn MS (2006) Fine roots vs. needles: a comparison of <sup>13</sup>C and <sup>15</sup>N dynamics in a ponderosa pine forest soil. *Biogeochemistry* 79(3):361–382
- Brunn M, Hafner BD, Zwetsloot MJ, Weikl F, Pritsch K, Hikino K, Ruehr NK, Sayer EJ, Bauerle TL (2022) Carbon allocation to root exudates is maintained in mature temperate tree species under drought. *New Phytol* 235(3):965–977
- Chen X, Maignan F, Viovy N, Bastos A, Goll D, Wu J, Liu L, Yue C, Peng S, Yuan W, da Conceição AC, O'Sullivan M, Ciais P (2020) Novel representation of leaf phenology improves simulation of Amazonian evergreen forest photosynthesis in a land surface model. *J Adv Model Earth Sy* 12(1):e2018MS001565
- Cheng L, Zhang L, Wang YP, Yu Q, Eamus D (2014) Quantifying the effects of elevated CO<sub>2</sub> on water budgets by combining FACE data with an ecohydrological model. *Ecohydrology* 7(6):1574–1588
- da Costa AC, Metcalfe DB, Doughty CE, de Oliveira AA, Neto GF, da Costa MC, Silva Junior Jda, Aragão LE, Almeida S, Galbraith DR (2014) Ecosystem respiration and net primary productivity after 8–10 years of experimental through-fall reduction in an eastern Amazon forest. *Plant Ecol Divers* 7(1–2):7–24
- De Kauwe MG, Medlyn BE, Zaehle S, Walker AP, Dietze MC, Hickler T, Jain AK, Luo Y, Parton WJ, Prentice IC (2013) Forest water use and water use efficiency at elevated CO<sub>2</sub>: a model-data intercomparison at two contrasting temperate forest FACE sites. *Global Change Biol* 19(6):1759–1779
- De Kauwe MG, Medlyn BE, Zaehle S, Walker AP, Dietze MC, Wang YP, Luo Y, Jain AK, El-Masri B, Hickler T (2014) Where does the carbon go? A model-data intercomparison of vegetation carbon allocation and turnover processes at two temperate forest free-air CO<sub>2</sub> enrichment sites. *New Phytol* 203(3):883–899
- Donohue RJ, McVICAR TR, Roderick ML (2009) Climate-related trends in Australian vegetation cover as inferred from satellite observations, 1981–2006. *Global Change Biol* 15(4):1025–1039
- FAO (2012) Global ecological zones for FAO forest reporting: 2010 update. FAO Forestry Paper 179. FAO, Rome, Italy
- Feng Y-L, Li X (2007) The combined effects of soil moisture and irradiance on growth, biomass allocation, morphology and photosynthesis in *Amorpha villosa*. *Agroforest Syst* 71(2):89–98
- Franck N, Winkler S, Pastenes C, Infante R (2007) Acclimation to sun and shade of three accessions of the Chilean native berry-crop murta. *Agroforest Syst* 69(3):215–229
- Friedlingsstein P, Joel G, Field CB, Fung IY (1999) Toward an allocation scheme for global terrestrial carbon models. *Global Change Biol* 5(7):755–770
- Global Modeling and Assimilation Office (2004) File Specification for Goddard Earth Observing System Data Assimilation System (GEOSDAS) Gridded Output Version 5.3, Report. NASA Goddard Space Flight Cent, Greenbelt, MD
- Hui D, Jackson RB (2006) Geographical and interannual variability in biomass partitioning in grassland ecosystems: a synthesis of field data. *New Phytol* 169(1):85–93
- Ikegami M, Whigham DF, Werger MJ (2007) Responses of rhizome length and ramet production to resource availability in the clonal sedge *Scirpus olneyi* A. Gray. *Plant Ecol* 189(2):247–259
- Ise T, Litton CM, Giardina CP, Ito A (2010) Comparison of modeling approaches for carbon partitioning impact on estimates of global net primary production and equilibrium biomass of woody vegetation from MODIS GPP. *J Geophys Res Biogeosci* 115:G04025. <https://doi.org/10.1029/2010JG001326>
- Iszkuło G, Boratyński A (2004) Interaction between canopy tree species and European yew *Taxus baccata* (Taxaceae). *Polish J Ecol* 52(4):523–531
- Iszkuło G, Boratyński A (2006) Analysis of the relationship between photosynthetic photon flux density and natural *Taxus baccata* seedlings occurrence. *Acta Oecol* 29(1):78–84
- Keeling CD, Whorf TP (2005) Atmospheric CO<sub>2</sub> records from sites in the SIO air sampling network. In: Trends: A Compendium of Data on Global Change.

- Carbon Dioxide Information Analysis Center, Oak Ridge National Laboratory, U.S. Department of Energy, Oak Ridge.
- Kobe RK, Iyer M, Walters MB (2010) Optimal partitioning theory revisited: nonstructural carbohydrates dominate root mass responses to nitrogen. *Ecology* 91(1):166–179
- Krinner G, Viovy N, de Noblet-Ducoudré N, Ogée J, Polcher J, Friedlingstein P, Ciais P, Sitch S, Prentice IC (2005) A dynamic global vegetation model for studies of the coupled atmosphere-biosphere system. *Global Biogeochem Cycles* 19:GB1015. <https://doi.org/10.1029/2003GB002199>
- Lapenis AG, Lawrence GB, Heim A, Zheng C, Shortle W (2013) Climate warming shifts carbon allocation from stemwood to roots in calcium-depleted spruce forests. *Global Biogeochem Cycles* 27(1):101–107
- Lawrence PJ, Feddesma JJ, Bonan GB, Meehl GA, O'Neill BC, Oleson KW, Levis S, Lawrence DM, Kluzek E, Lindsay K (2012) Simulating the biogeochemical and biogeophysical impacts of transient land cover change and wood harvest in the community climate system model (CCSM4) from 1850 to 2100. *J Clim* 25(9):3071–3095
- Luyssaert S, Jammot M, Stoy PC, Estel S, Pongratz J, Ceschia E, Churkina G, Don A, Erb K, Ferlicoq M (2014) Land management and land-cover change have impacts of similar magnitude on surface temperature. *Nat Clim Change* 4(5):389–393
- Matzek V (2011) Superior performance and nutrient-use efficiency of invasive plants over non-invasive congeners in a resource-limited environment. *Biol Invasions* 13(12):3005–3014
- McCarthy M, Enquist B (2007) Consistency between an allometric approach and optimal partitioning theory in global patterns of plant biomass allocation. *Funct Ecol* 21(4):713–720
- McCarthy HR, Oren R, Johnsen KH, Gallet-Budynek A, Pritchard SG, Cook CW, LaDeau SL, Jackson RB, Finzi AC (2010) Re-assessment of plant carbon dynamics at the Duke free-air CO<sub>2</sub> enrichment site: interactions of atmospheric [CO<sub>2</sub>] with nitrogen and water availability over stand development. *New Phytol* 185(2):514–528
- McMurtrie RE, Dewar RC (2013) New insights into carbon allocation by trees from the hypothesis that annual wood production is maximized. *New Phytol* 199(4):981–990
- Myneni RB, Yang W, Nemani RR, Huete AR, Dickinson RE, Knyazikhin Y, Didan K, Fu R, Juárez RIN, Saatchi SS (2007) Large seasonal swings in leaf area of Amazon rainforests. *Proc Natl Acad Sci USA* 104(12):4820–4823
- Nelson JA, Morgan JA, LeCain DR, Mosier AR, Milchunas DG, Parton BA (2004) Elevated CO<sub>2</sub> increases soil moisture and enhances plant water relations in a long-term field study in semi-arid shortgrass steppe of Colorado. *Plant Soil* 259(1–2):169–179
- Norby RJ, Warren JM, Iversen CM, Medlyn BE, McMurtrie RE (2010) CO<sub>2</sub> enhancement of forest productivity constrained by limited nitrogen availability. *Proc Natl Acad Sci USA* 107(45):19368–19373
- Peng Y, Guo D, Yang Y (2017) Global patterns of root dynamics under nitrogen enrichment. *Global Ecol Biogeogr* 26(1):102–114
- Perrin PM, Mitchell FJ (2013) Effects of shade on growth, biomass allocation and leaf morphology in European yew (*Taxus baccata* L.). *Eur J Forest Res* 132(2):211–218
- Piao S, Wang X, Park T, Chen C, Lian X, He Y, Bjerke JW, Chen A, Ciais P, Tømmervik H (2020) Characteristics, drivers and feedbacks of global greening. *Nat Rev Earth Env* 1(1):14–27
- Poorter L (1999) Growth responses of 15 rain-forest tree species to a light gradient: the relative importance of morphological and physiological traits. *Funct Ecol* 13(3):396–410
- Poorter H, Niklas KJ, Reich PB, Oleksyn J, Poot P, Mommer L (2012) Biomass allocation to leaves, stems and roots: meta-analyses of interspecific variation and environmental control. *New Phytol* 193(1):30–50
- Potter CS, Randerson JT, Field CB, Matson PA, Vitousek PM, Mooney HA, Klooster SA (1993) Terrestrial ecosystem production: a process model based on global satellite and surface data. *Global Biogeochem Cycles* 7(4):811–841
- Samaniego L, Thober S, Kumar R, Wanders N, Rakovec O, Pan M, Zink M, Sheffield J, Wood EF, Marx A (2018) Anthropogenic warming exacerbates European soil moisture droughts. *Nat Clim Change* 8(5):421–426
- Scheiter S, Higgins SI (2009) Impacts of climate change on the vegetation of Africa: an adaptive dynamic vegetation modelling approach. *Global Change Biol* 15(9):2224–2246
- Sharpe PJ, Rykiel Jr EJ (1991) Modelling integrated response of plants to multiple stresses. In: Mooney HA, Winner WE, Pell EJ (eds) *Response of plants to multiple stresses*. Academic Press, San Diego, pp 205–224
- Shen M, Piao S, Jeong S-J, Zhou L, Zeng Z, Ciais P, Chen D, Huang M, Jin C-S, Li LZ (2015) Evaporative cooling over the Tibetan Plateau induced by vegetation growth. *Proc Natl Acad Sci USA* 112(30):9299–9304
- Sierra CA, Ceballos-Núñez V, Hartmann H, Herrera-Ramírez D, Metzler H (2022) Ideas and perspectives: Allocation of carbon from net primary production in models is inconsistent with observations of the age of respired carbon. *Biogeosciences* 19(16):3727–3738
- Townsend AR, Vitousek PM, Trumbore SE (1995) Soil organic matter dynamics along gradients in temperature and land use on the island of Hawaii. *Ecology* 76(3):721–733
- Wan S, Norby RJ, Pregitzer KS, Ledford J, O'Neill EG (2004) CO<sub>2</sub> enrichment and warming of the atmosphere enhance both productivity and mortality of maple tree fine roots. *New Phytol* 162(2):437–446
- Wang GG, Bauerle WL, Mudder BT (2006) Effects of light acclimation on the photosynthesis, growth, and biomass allocation in American chestnut (*Castanea dentata*) seedlings. *For Ecol Manage* 226(1):173–180
- Wang Y, Law R, Pak B (2010) A global model of carbon, nitrogen and phosphorus cycles for the terrestrial biosphere. *Biogeosciences* 7(7):2261–2282
- Wang Q, Yan G, Luo X, Liu G, Wang H, Xing Y (2023) Symbiotic mycorrhizal types affect patterns of tree aboveground and belowground C allocation in Northeast China. *Ecol Process* 12:26
- Ward EJ, Oren R, Bell DM, Clark JS, McCarthy HR, Kim H-S, Domec J-C (2013) The effects of elevated CO<sub>2</sub> and nitrogen fertilization on stomatal conductance estimated from 11 years of scaled sap flux measurements at Duke FACE. *Tree Physiol* 33(2):135–151
- Waring RH (1991) Responses of evergreen trees to multiple stresses. In: Mooney HA, Winner WE, Pell EJ (eds) *Response of plants to multiple stresses*. Academic Press, San Diego, pp 371–390
- Wei N, Xia J, Zhou J, Jiang L, Cui E, Ping J, Luo Y (2022) Evolution of uncertainty in terrestrial carbon storage in earth system models from CMIP5 to CMIP6. *J Clim* 35(17):5483–5499
- Xia J, Chen Y, Liang S, Liu D, Yuan W (2015) Global simulations of carbon allocation coefficients for deciduous vegetation types. *Tellus B Chem Phys Meteorol* 67:28016
- Xia J, Yuan W, Wang Y-P, Zhang Q (2017) Adaptive carbon allocation by plants enhances the terrestrial carbon sink. *Sci Rep* 7(1):3341
- Xia J, Yuan W, Lienert S, Joos F, Ciais P, Viovy N, Yp W, Wang X, Zhang H, Chen Y (2019) Global patterns in net primary production allocation regulated by environmental conditions and forest stand age: a model-data comparison. *J Geophys Res Biogeosci* 124(7):2039–2059
- Xu R, Prentice I (2008) Terrestrial nitrogen cycle simulation with a dynamic global vegetation model. *Global Change Biol* 14(8):1745–1764
- Xu X, Niu S, Sherry R, Zhou X, Zhou J, Luo Y (2012) Interannual variability in responses of belowground NPP and NPP partitioning to long-term warming and clipping in a tallgrass prairie. *Global Change Biol* 18:1648–1656
- Xu W, Yuan W, Dong W, Xia J, Liu D, Chen Y (2013) A meta-analysis of the response of soil moisture to experimental warming. *Environ Res Lett* 8:044027
- Xu Z, Ren H, Li M-H, Brunner I, Yin J, Liu H, Kong D, Lü X-T, Sun T, Cai J (2016) Experimentally increased water and nitrogen affect root production and vertical allocation of an old-field grassland. *Plant Soil* 412:369–380
- Yuan W, Liu S, Dong W, Liang S, Zhao S, Chen J, Xu W, Li X, Barr A, Black TA (2014) Differentiating moss from higher plants is critical in studying the carbon cycle of the boreal biome. *Nat Commun* 5:4270. <https://doi.org/10.1038/ncomms5270>
- Zhang Q, Wang Y, Pitman A, Dai Y (2011) Limitations of nitrogen and phosphorus on the terrestrial carbon uptake in the 20th century. *Geophys Res Lett* 38:L22701. <https://doi.org/10.1029/2011GL049244>
- Zhu Z, Piao S, Myneni RB, Huang M, Zeng Z, Canadell JG, Ciais P, Sitch S, Friedlingstein P, Arneeth A (2016) Greening of the Earth and its drivers. *Nat Clim Change* 6:791–795

## Publisher's Note

Springer Nature remains neutral with regard to jurisdictional claims in published maps and institutional affiliations.